Supporting Information

A Cathode Interlayer Based on Indandione-Terminated Quinoidal Compound Enables 19% Efficiency Binary Organic Solar Cells

Content

1. Measurements

^{1}H NMR and ^{13}C NMR spectra were measured on a Bruker 400 MHz spectrometer in chloroform-*d* ($CDCl_3$) with tetramethylsilane (TMS) as internal standard at room temperature. Matrix-assisted laser desorption ionization time-of-light (MALDI-TOF) mass spectra were recorded on a Bruker/AutoflexIII Smartbean MALDI mass spectrometer with 2-[(2*E*)-3-(4-tert-buthylphenyl)-2-methylprop-2-enylodene]malononitrile (DCTB) as the matrix in a reflection mode. Thermogravimetric analysis (TGA) was carried out on a TA Q50 thermogravimetric analyzer with the heating rate of 10 °C min^{-1} at a nitrogen flow. Ultraviolet-visible-near-infrared (UV-*vis*-NIR) absorption spectra were measured on a Shimadzu UV-3600 plus spectrometer. Time-dependent in-situ UV-*vis*-NIR spectra was conducted on a DU-300 dynamic spectrometer in transmission mode with a time interval of 0.05 s from Shaanxi Puguangweishi Technology Co., Ltd. Cyclic voltammetry (CV) were measured in anhydrous dichloromethane using a CHI660 electrochemical analyzer with a three-electrode cell at a scan rate of 100 mV s^{-1}. Terabutylammonium hexafluorophosphate (Bu_4NPF_6, 0.1 mol L^{-1}) was used as the supporting electrolyte. A Pt disk with 2 mm diameter, a Pt wire and a saturated calomel electrode (SCE) were used as working, counter and reference electrodes, respectively. Ferrocene/ferrocenium (Fc/Fc^+) was measured under the same conditions for calibration. which was 0.41 V *versus* SCE. The LUMO energy level was calculated according to the equation of $E_{LUMO} = -(4.39 + E^{re}_{onset})$ eV, where E^{re}_{onset} is the reduction onset-potentials against SCE. Ultroviolet photoelectron spectrometer (UPS) measurements were carried out by using a VG Escalabmkll spectrometer (UK) with He I (21.2 eV) discharge lamp excitation. Electron paramagnetic resonance (EPR) spectroscopy was conducted on a JEOL JESFA200 spectrometer at room temperature. Grazing incidence X-ray diffraction (GIXRD) was measured by a Rigaku Smart Lab with Cu Kα source (λ = 1.54056 Å) in air. The thickness of films was measured by Dektak 150 profilometer. Atomic force microscopy (AFM) measurements were performed in a tapping mode on a Bruker

MultiMode 8 instrument. The C-V characteristics of the Mott-Schottky analysis were measured by applying a low alternating current (AC) perturbation signal with a fixed frequency and sweeping the direct current (DC) bias. VOC versus light intensity, photo CELIV and transient photovoltage (TPV) measurements were performed using the commercially available Paios system (FLUXiM AG, Switzerland).

2. Theoretical calculations

All the theoretical calculations were performed with a Gaussian 09 program[1].

The NICS analysis was based on the single crystal analysis. The aromaticity of each ring was measured by nucleus-independent chemical shift (NICS), which was computed using the gauge invariant atomic orbital (GIAO)[2] approach at the GIAO-B3LYP/def2-SVP level of theory.[2-3] ACID plot was calculated by using the method developed by Herges at CSGT-B3LYP/def2-SVP.[4]

The calculations of complexation energy and LUMO distribution were calculated by DFT, with the optimized molecular geometries of dimers at the B3LYP/6-31G(d, p). For simplifying, the side chains were replaced with methyl groups. The corresponding intermolecular complexation energies were calculated by correction of the basis set super position error (BSSE) according to the literature method.

Natural orbital occupation number (NOON) calculations were done by spin unrestricted UCAM-B3LYP/6-31G (d, p) method and the diradical character (y_0) was calculated according to Yamaguchi's scheme: $y_0 = 1 - (2T/(1 + T^2))$, and T = (nHOMO – nLUMO)/2. nHOMO is the occupation number of the HOMO, nLUMO is the occupation number of the LUMO.

The charge transfer integrals for the molecular dimer extracted from the experimental crystal structures were calculated at M06-2X/Def2-SVP level in the CT module of NWchem package.

3. Spin density calculation

The spin densities of CILs are evaluated using a commonly used reagent 2,2,6,6-

tetramethylpiperidinium-nitrogen-oxide (TEMPO) as a reference. One TEMPO molecule possesses one radical.

(1) The spins of TEMPO, X_0, can be calculated as: $X_0 = \frac{m_0}{M_0} \times N_A$, where M_0 represents the molecular weight of TEMPO (156.28 g/mol), m_0 is the weight of TEMPO used in the EPR measurement, and I_0 is the quadratic integral intensity of the spin signal in EPR spectrum of TEMPO, and N_A is Avogadro's constant.

(2) The spins of CIL, X, can be calculated as: $X = \frac{X_0}{I_0} \times I$, where I is the quadratic integral intensity of the spin signal in EPR spectrum of CIL.

(3) The spin density of CIL can be calculated as: $spin\ density = \frac{X}{V} = \frac{X\rho}{m}$, where m is the weight of CIL used in EPR measurement, and the density $\rho \approx 1$ g/cm^3.

4. Organic solar cells (OSCs) fabrication and characterization

Fabrication of the conventional structure devices: The OSCs device architecture was ITO/PEDOT:PSS/active layers/CILs/Ag. Patterned ITO substrates were cleaned with detergent water, deionized water, acetone and ethyl alcohol in an ultrasonic bath sequentially for 15 min. The pre-cleaned ITO-coated glass substrates were UV/ozone-treated for 15 min. PEDOT:PSS (4083) was purchased from the Clevios and spin-coated on ITO substrate. The active layer of D18:L8-BO (D/A 1:1.3) was dissolved in chloroform (CF) at the concentration of 5.5 mg mL^{-1} (for polymer) with 1,8-diiodooctane (0.25%, v/v) as the additive. The solution was stirred for 1 h at 40 ^{o}C and then spin-coated (3500 rpm for 30 s) on the top of PEDOT:PSS in a nitrogen filled glove box. The active layer was then thermal annealed at 100 °C for 10 min. PDINN or Q6P dissolved in methanol at a concentration of 1 mg mL^{-1} was spin-coated onto the active layer at 3000 rpm for 30 s. Finally, about 100 nm Ag was deposited by thermal evaporation through a shadow mask under a high vacuum of 1× 10^{-5} Pa. The current density-voltage (*J-V*) curves of the OSCs were measured by metal masking of 0.04 cm^2

via the AAA solar simulator (SS-F5-3A, Enli Technology Co. Ltd, Taiwan) along with AM 1.5G spectra, whose intensity was calibrated by the certified standard silicon solar cell at 100 mW/cm^2. The external quantum efficiencies (EQE) spectra were measured through the Solar Cell Spectral Response Measurement System QE-R3011 (Enli Technology Co. Ltd, Taiwan).

Fabrication of the electron-only devices: The devices structure is ITO/ZnO/L8-BO/PDINN or Q6P/Ag. The ITO-coated glass substrates were washed as mentioned above. Sol-gel ZnO were spin-coated on the ITO substrates and annealed at 200 °C for 1 hour in air. L8-BO was dissolved in chloroform (15 mg mL^{-1}) and spin-coated on the top of ZnO. Afterwards, PDINN or Q6P methanol solution was spin-coated. Finally, 100 nm thick of Ag layer were deposited under a high vacuum of 1× 10^{-5} Pa. The electron mobilities were approximated by the Mott-Gurney equation: $J = 9\varepsilon_0\varepsilon_r\mu V^2/8L^3$, where J is the current density, ε_0 is the permittivity of free space, ε_r is the permittivity of the organic materials, μ is the electron mobility, V is the effective voltage and L is the film thickness of the neat film.

5. Materials and synthetic procedures

Chemical reagents were purchased from Energy-Chemical, Innochem or Aldrich, and used as received unless otherwise noted. All air and water sensitive reactions were performed under argon atmosphere.

Synthetic procedures

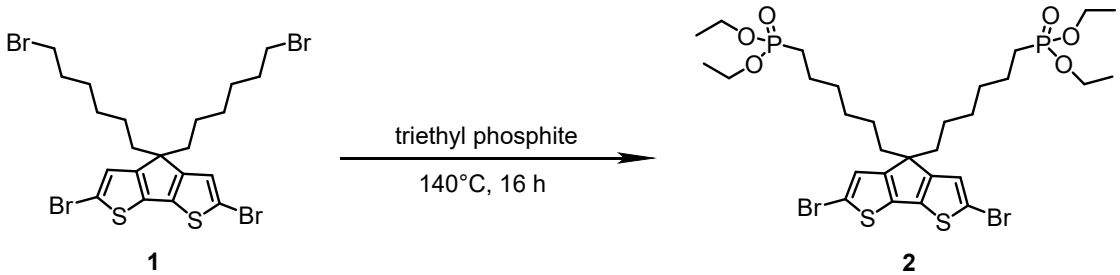

Scheme S1. The synthetic route to compound **2**.

Synthesis of compound 2: The mixture of compound **1** (1 g, 1.51 mmol) and triethyl

phosphite (10 mL) was stirred at 140 °C for 16 hours. After removal of triethyl phosphite, the crude product was purified by chromatography on silica gel using EA/DCM/MeOH = 5/1/1 (V/V/V) as the eluent, affording compound **2** as a yellow liquid (0.80 g, yield:68%). ^{1}H NMR (400 MHz, $CDCl_3$, δ): 6.90 (d, J = 5.2 Hz, 2H), 4.06 (m, J = 5.2 Hz, 8H), 1.76 (t, J = 6.8 Hz, 4H), 1.65 (m, 4H), 1.50 (m, 4H), 1.30 (m, 4H), 1.24 (m, 16H), 1.13 (m, 4H), 0.87 (m, 4H). ^{13}C NMR (100 MHz, $CDCl_3$, δ) 155.44, 136.01, 124.24, 111.01, 61.20, 54.78, 37.18, 29.93, 28.98, 28.98, 25.80, 23.86,21.98, 19.18, 17.71, 16.27. MS (MALDI-TOF): Calcd for $C_{29}H_{46}Br_2O_6P_2S_2$ $[M]^+$: 776.0600, found: 776.0600.

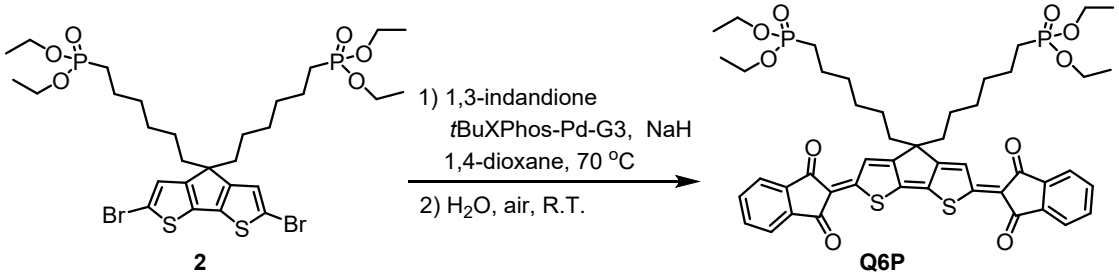

Scheme S2. The synthetic route to Q6P.

Synthesis of compound Q6P: The solution of **2** (500 mg, 0.64 mmol), 1,3-indanedione (225 mg, 1.55 mmol), *t*BuXPhos-Pd-G3 (10.23 mg, 12.88 μmol) and sodium hydride (60% dispersion in mineral oil, 118 mg, 2.96 mmol) in 1,4-dioxane (7.5 mL) was stirred at 70 °C for 1.5 h in the absence of light. Subsequently, 10 mL deionized water and 10 mL DCM was added, and the mixture was stirred in air for 30 min. The organic layer was washed with water, brine and dried over anhydrous $MgSO_4$. After removal of the solvent, the crude product was purified by chromatography on silica gel using EA:DCM:MeOH= 3/3/1 (V/V/V) as the eluent, affording Q6P as a purple solid (116 mg, yield: 20%). ^{1}H NMR (400 MHz, $CDCl_3$, δ): δ 8.04 (s, 2H), 7.93 (m, 4H), 7.76 (m, 4H), 4.06 (m, 8H), 2.03 (m, 4H), 1.67 (m, 4H) 1.47 (m, 4H), 1.30 (m, 20H), 1.07 (m, 4H). ^{13}C NMR (100 MHz, $CDCl_3$, δ) 189.96, 187.53, 175.61, 164.98, 150.92, 141.53, 140.95, 134.79, 123.01, 120.41, 119.50, 61.56, 52.00, 39.08, 29.93, 28.98, 25.80, 23.86,21.98, 19.18, 17.71, 16.27. MS (MALDI-TOF): Calcd for $C_{47}H_{54}O_{10}P_2S_2$

$[M+H]^+$: 905.2634, found: 905.2633.

6. Supplementary Date

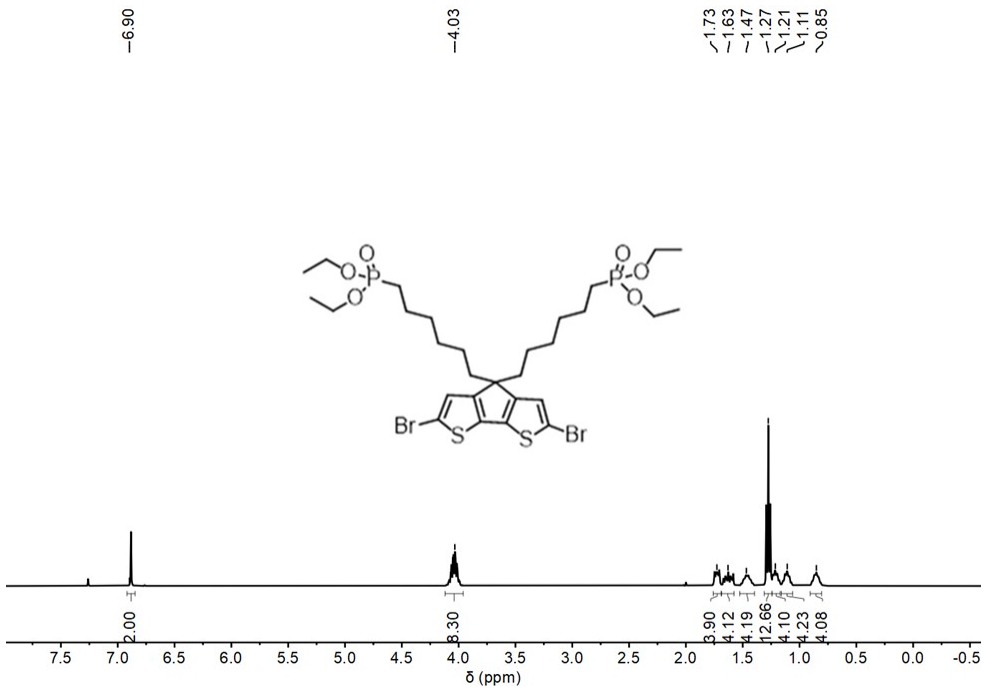

Figure S1. ^{1}H NMR spectrum of compound **2** (400 MHz, $CDCl_3$).

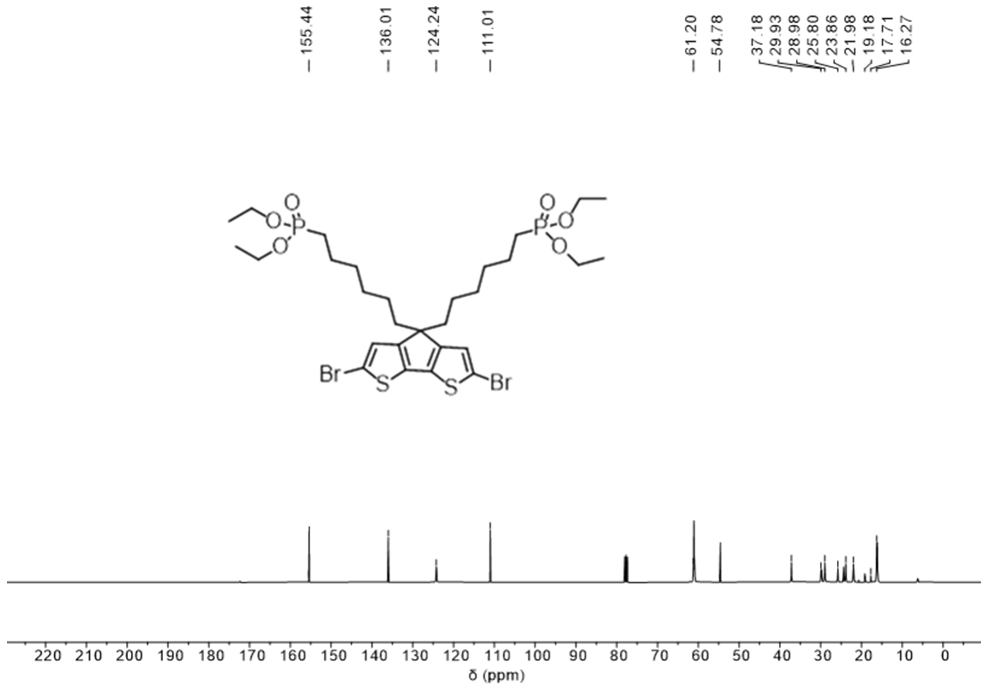

Figure S2. ^{13}C NMR spectrum of compound **2** (100 MHz, $CDCl_3$).

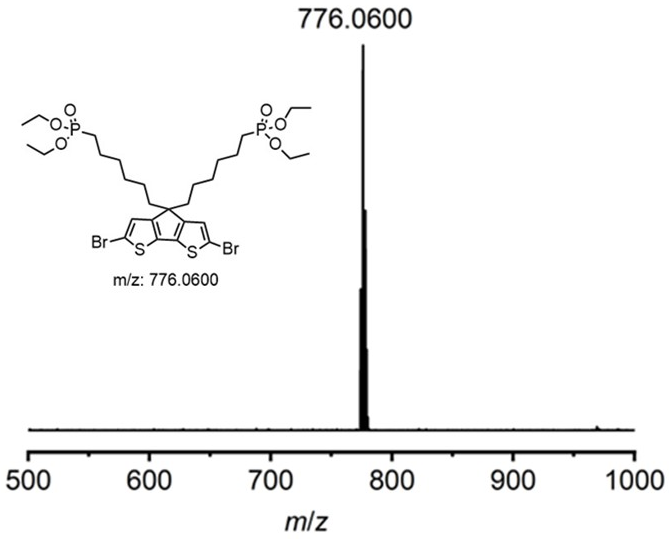

Figure S3. High-resolution MALDI-TOF mass spectra of compound **2**.

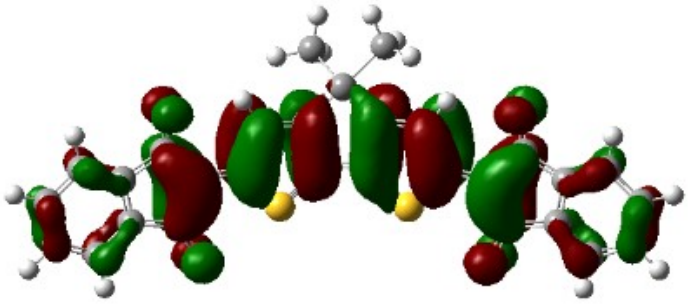

Figure S4. The LUMO distribution of Q6P.

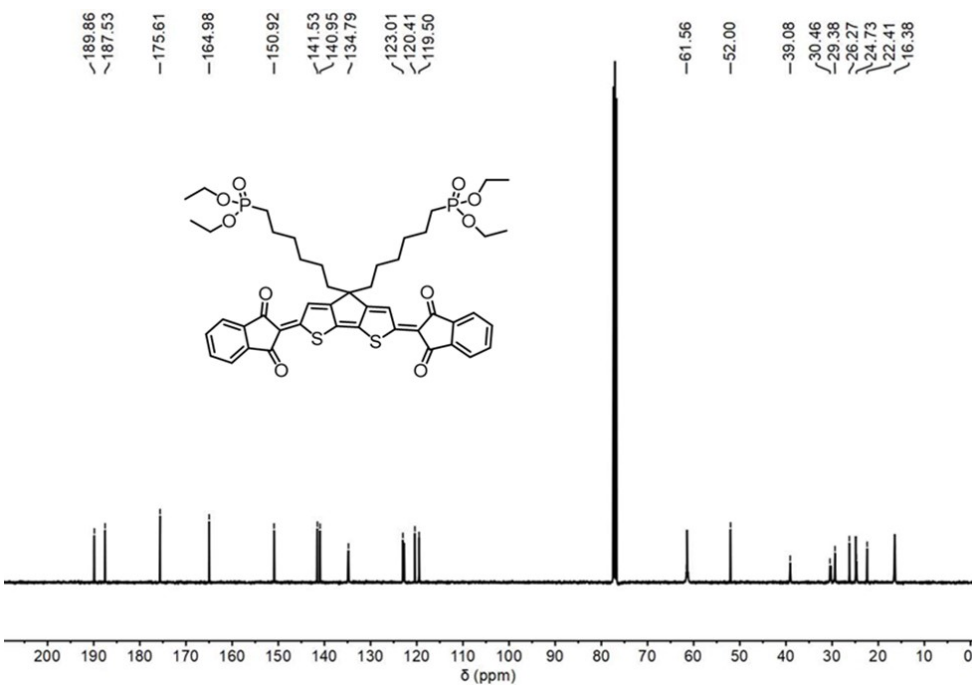

Figure S5. ^{13}C NMR spectrum of Q6P (100 MHz, $CDCl_3$).

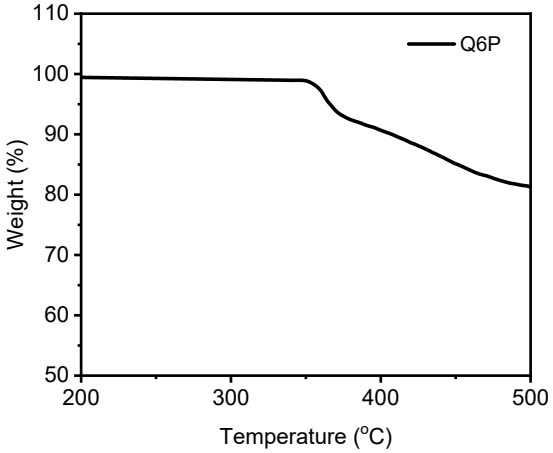

Figure S6. TGA curve of Q6P.

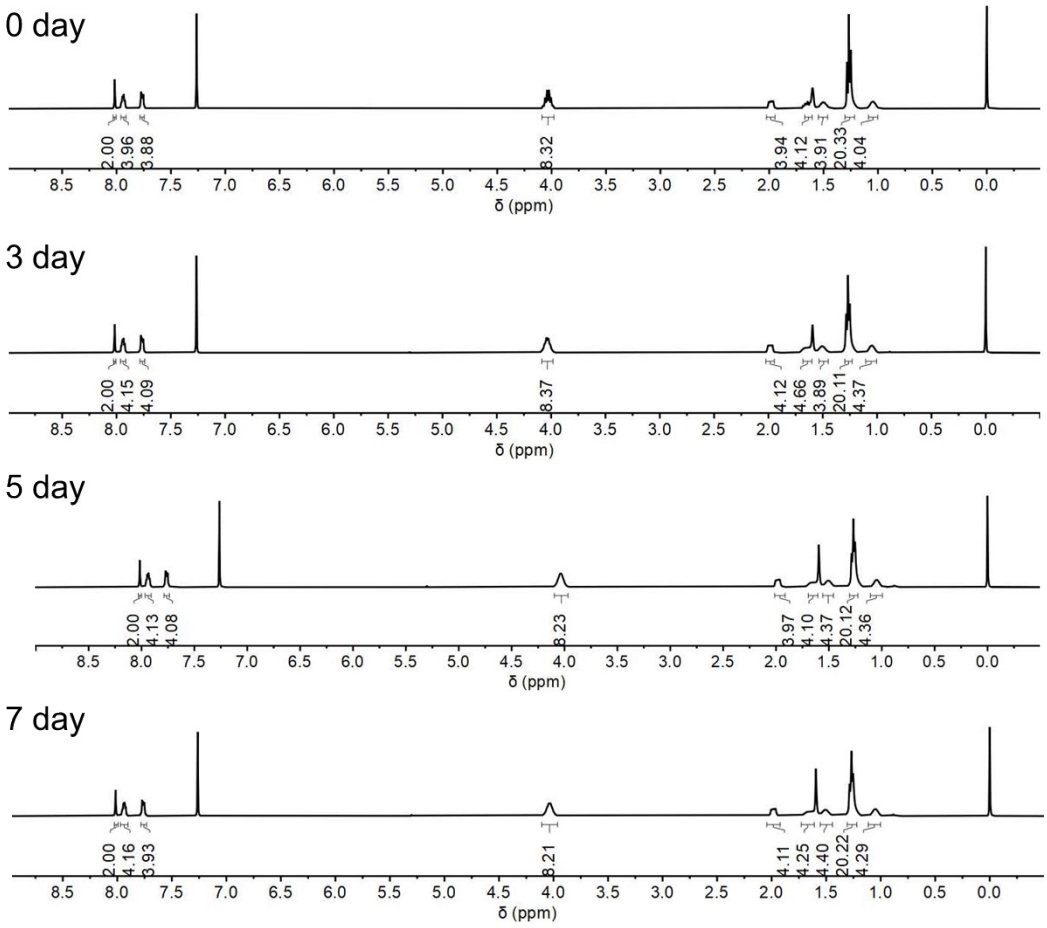

Figure S7. Variable-time ^{1}H NMR spectra of compound Q6P (400 MHz, $CDCl_3$).

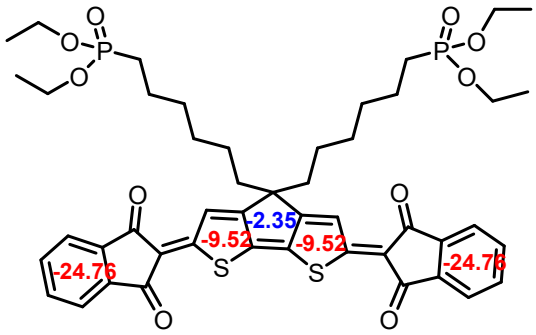

Figure S8. Calculated NICS values of Q6P.

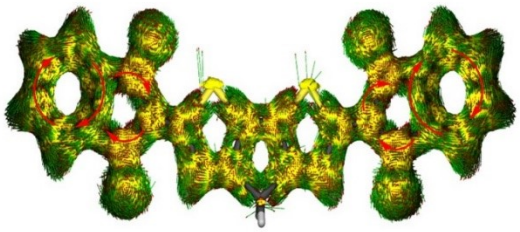

Figure S9. Calculated ACID plot of Q6P.

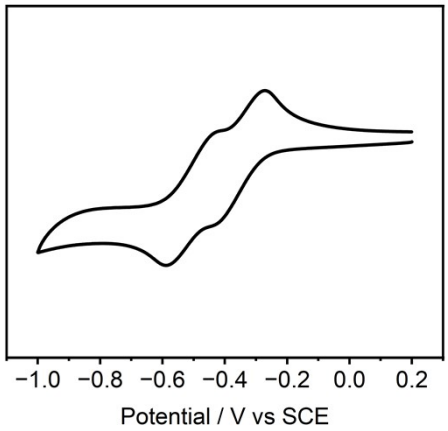

Figure S10. Solution cyclic voltammetry of Q6P.

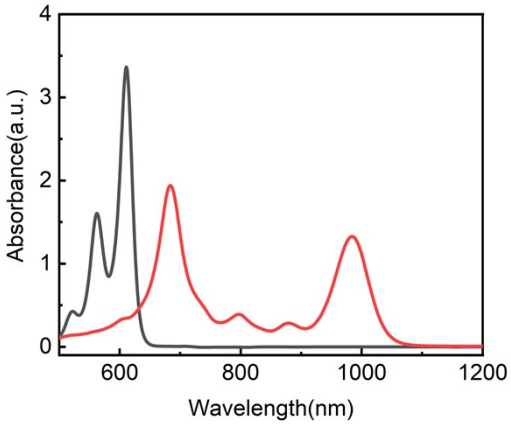

Figure S11. The absorption spectra of Q6C (black) and its radical anion (red) reduced by 1 equivalent of $TBABH_4$.

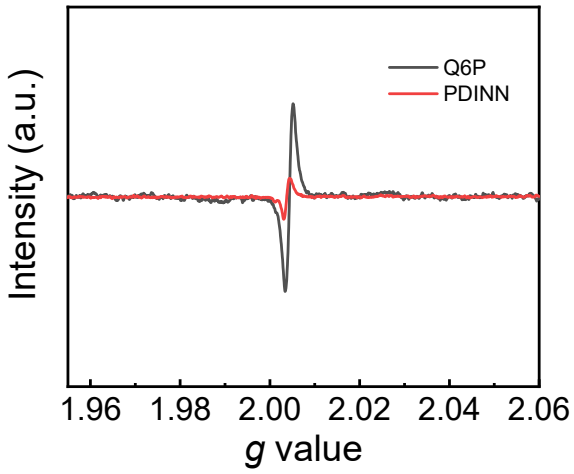

Figure S12. EPR spectrum of Q6P and PDINN thin films.

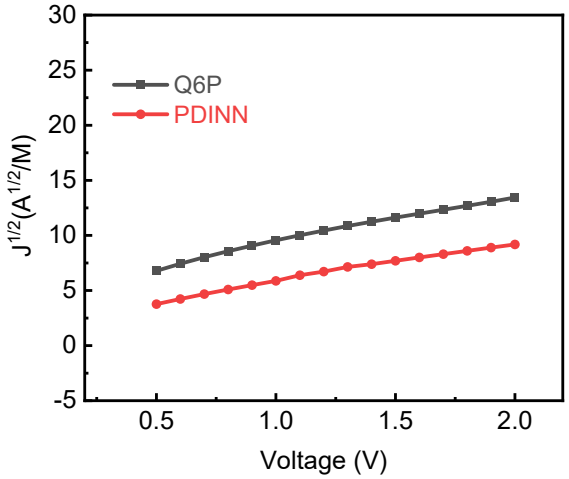

Figure S13. Electron mobility characteristic curve of Q6P and PDINN.

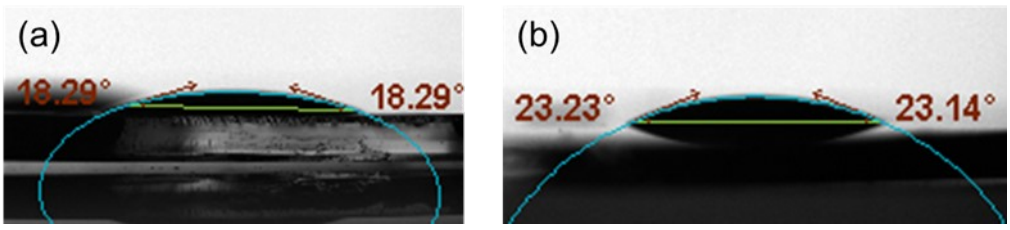

Figure S14. Contact angle for methanol solutions of Q6P (a) and PDINN (b) on the surface of active layer D18:L8BO.

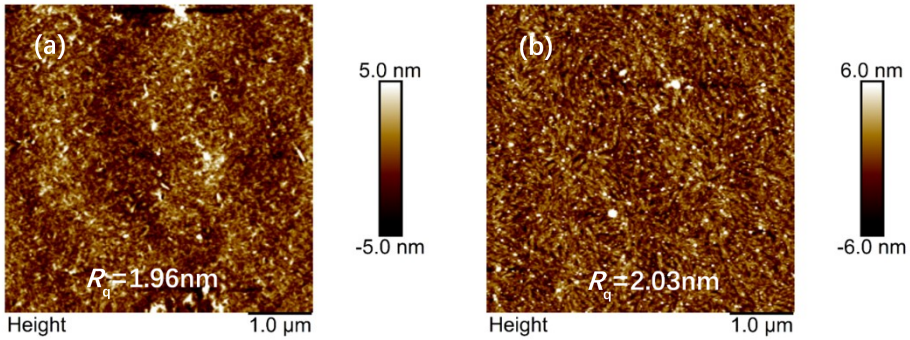

Figure S15. Atomic force microscopy height images (5 μm × 5 μm) of Q6P thin film on the (a) substrate and (b) on the active layer.

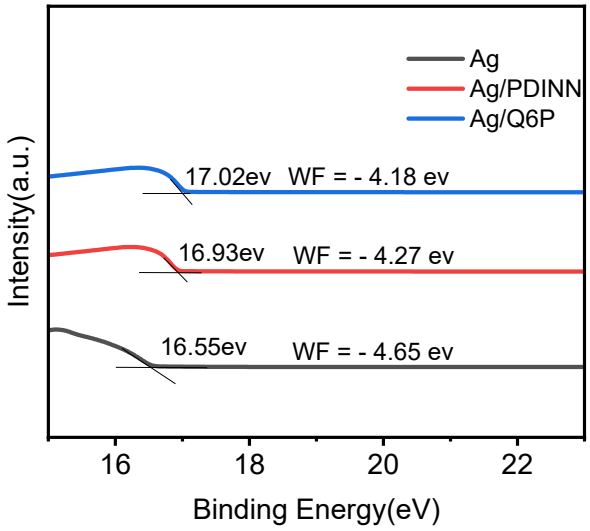

Figure S16. UPS spectra of the Ag electrodes covered with PDINN and Q6P.

6 X-ray crystallography

The single crystals of compound Q6P was grown by vapor-diffusion of hexane into chloroform solution. The data were collected on a “Bruker APEX-II CCD” diffractometer. In the Olex2, the structure was solved with the ShelXT structure solution program using Intrinsic Phasing and refined with the ShelXL refinement package using Least Squares minimisation.

Table S1. Crystal data and structure refinement for compound Q6P.

Identification code	Q6P	
Empirical formula	C47 H54 O10 P2 S2	
Formula weight	904.96	
Temperature	170.00 K	
Wavelength	1.34139 Å	
Crystal system	Triclinic	
Space group	P-1	
Unit cell dimensions	a = 10.742(3) Å	a= 112.731(13)°.
	b = 19.392(6) Å	b= 90.393(9)°.
	c = 24.568(5) Å	g = 102.666(10)°.
Volume	4581(2) $Å^3$	
Z	4	
Density (calculated)	1.312 Mg/m^3	
Absorption coefficient	1.428 mm^{-1}	
F(000)	1912	
Crystal size	0.17 x 0.17 x 0.05 mm^3	
Theta range for data collection	3.246 to 54.877°.	
Index ranges	-12<=h<=13, -23<=k<=23, -29<=l<=29	
Reflections collected	71371	
Independent reflections	17131 [R(int) = 0.1349]	
Completeness to theta = 53.594°	98.7 %	
Absorption correction	Semi-empirical from equivalents	
Max. and min. transmission	0.7508 and 0.5509	
Refinement method	Full-matrix least-squares on F^2	
Data / restraints / parameters	17131 / 102 / 1127	
Goodness-of-fit on F^2	1.110	
Final R indices [I>2sigma(I)]	R1 = 0.1640, wR2 = 0.3380	
R indices (all data)	R1 = 0.2306, wR2 = 0.3736	
Extinction coefficient	0.0035(2)	
Largest diff. peak and hole	1.168 and -0.937 $e.Å^{-3}$	

[1] Gaussian 09, Revision E.01, M. J. Frisch, G. W. Trucks, H. B. Schlegel, G. E. Scuseria, M. A. Robb, J. R. Cheeseman, G. Scalmani, V. Barone, B. Mennucci, G. A. Petersson, H. Nakatsuji, M. Caricato, X. Li, H. P. Hratchian, A. F. Izmaylov, J. Bloino, G. Zheng, J. L. Sonnenberg, M. Hada, M. Ehara, K. Toyota, R. Fukuda, J. Hasegawa, M. Ishida, T. Nakajima, Y. Honda, O. Kitao, H. Nakai, T. Vreven, J. A. Montgomery, Jr., J. E. Peralta, F. Ogliaro, M. Bearpark, J. J. Heyd, E. Brothers, K. N. Kudin, V. N. Staroverov, R. Kobayashi, J. Normand, K. Raghavachari, A. Rendell, J. C. Burant, S. S. Iyengar, J. Tomasi, M. Cossi, N. Rega, J. M. Millam, M. Klene, J. E. Knox, J. B. Cross, V. Bakken, C. Adamo, J. Jaramillo, R. Gomperts, R. E. Stratmann, O. Yazyev, A. J. Austin, R. Cammi, C. Pomelli, J. W. Ochterski, R. L. Martin, K. Morokuma, V. G. Zakrzewski, G. A. Voth, P. Salvador, J. J. Dannenberg, S. Dapprich, A. D. Daniels, Ö. Farkas, J. B. Foresman, J. V. Ortiz, J. Cioslowski, S11 D. J. Fox, Gaussian, Inc., Wallingford CT, **2013**.

[2] S. Klod, E. Kleinpeter, J. Chem. Soc., Perkin Trans. 2, 2001, 1893-1898.

[3] Z. Liu, T. Lu, Q. Chen, Carbon, 2020, 165, 468-475.

[4] D. Geuenich, K. Hess, F. Köhler, R. Herges, Chem. Rev., 2005, 105, 3758-3772.